Radiation hardness of graphene and MoS2 field effect devices against swift heavy ion irradiation

O. Ochedowski, K. Marinov, G. Wilbs, G. Keller, N. Scheuschner, D. Severin, M. Bender, J. Maultzsch, F. J. Tegude, and M. Schleberger

Citation: Journal of Applied Physics **113**, 214306 (2013); doi: 10.1063/1.4808460
View online: http://dx.doi.org/10.1063/1.4808460
View Table of Contents: http://scitation.aip.org/content/aip/journal/jap/113/21?ver=pdfcov
Published by the AIP Publishing

Radiation hardness of graphene and MoS_2 field effect devices against swift heavy ion irradiation

O. Ochedowski,[1] K. Marinov,[1] G. Wilbs,[2] G. Keller,[2] N. Scheuschner,[3] D. Severin,[4] M. Bender,[4] J. Maultzsch,[3] F. J. Tegude,[2] and M. Schleberger[1,a)]
[1]*Fakultät für Physik and CeNIDE, Universität Duisburg-Essen, Lotharstr. 1, 47048 Duisburg, Germany*
[2]*Solid State Electronics Department and CeNIDE, University of Duisburg-Essen, Lotharstr. 55, 47048 Duisburg, Germany*
[3]*Institut für Festkörperphysik, Technische Universität Berlin, Hardenbergstr. 36, 10623 Berlin, Germany*
[4]*GSI Helmholtz Centre, Planckstr. 1, 64291 Darmstadt, Germany*

(Received 12 April 2013; accepted 17 May 2013; published online 7 June 2013)

We have investigated the deterioration of field effect transistors based on two-dimensional materials due to irradiation with swift heavy ions. Devices were prepared with exfoliated single layers of MoS_2 and graphene, respectively. They were characterized before and after irradiation with 1.14 GeV U^{28+} ions using three different fluences. By electrical characterization, atomic force microscopy, and Raman spectroscopy, we show that the irradiation leads to significant changes of structural and electrical properties. At the highest fluence of 4×10^{11} ions/cm^2, the MoS_2 transistor is destroyed, while the graphene based device remains operational, albeit with an inferior performance. © *2013 AIP Publishing LLC*. [http://dx.doi.org/10.1063/1.4808460]

I. INTRODUCTION

Immediately after its discovery, graphene was shown to be an excellent material for the fabrication of field effect devices.[1] Due to its ballistic transport properties, very large mobilities can be achieved at least under optimum conditions.[2,3] A graphene FET operating at GHz frequencies was reported by IBM researchers in 2008.[4] Because graphene is a gapless semiconductor, it shows an ambipolar behaviour, i.e., both charge carrier types contribute to its conductivity. Therefore, researchers focussed on other possible 2D materials which have a bandgap, and in 2011, the first high performance field effect device with single layer MoS_2 was realized.[5] This two-dimensional (2D) material has a lower carrier mobility but also bandgap of ≈1.8 eV (Ref. 6) and thus a MoS_2-FET can be operated with large off-on current ratios.[7] Both materials are thus promising candidates for use in future electronics.[8–11] In this paper, we study whether such devices are sensitive to radiation by swift heavy ions (SHI). The reason for this study is two-fold: SHI are a well-known tool for material modification[12,13] and might thus be useful to manipulate 2D-FETs as well. In addition, this type of projectile interacts with solids primarily via electronic excitations and offer thus the unique chance to study how 2D materials react to ionizing particle irradiation. This is not only interesting for basic science but represents also an important issue if 2D-FETs are to be operational in ionizing environments as, e.g., in outer space.

II. EXPERIMENT

A. Experimental details

For this experiment, simple field effect devices (called FETs in the following) were prepared from single layer graphene (SLG) as well as from single layer MoS_2 (SLM). The first step is mechanical exfoliation from single crystals onto 90 nm SiO_2 on a Si wafer (*p*-doped, $\rho = (0.001 - 0.005)\,\Omega$cm). The second step is selection of appropriate flakes and determination of their layer number with μ-Raman spectroscopy.[14] In a third step, selected SLG and SLM are contacted using photolithography and vacuum evaporation. Two gold contacts (with Ti as bonding agent) serve as source and drain, the Si substrate as a global back-gate, see Fig. 1.

Typical channel length and width of our devices are $L = 6\,\mu$m and $W = (3 - 12)\,\mu$m. Step four is the electrical

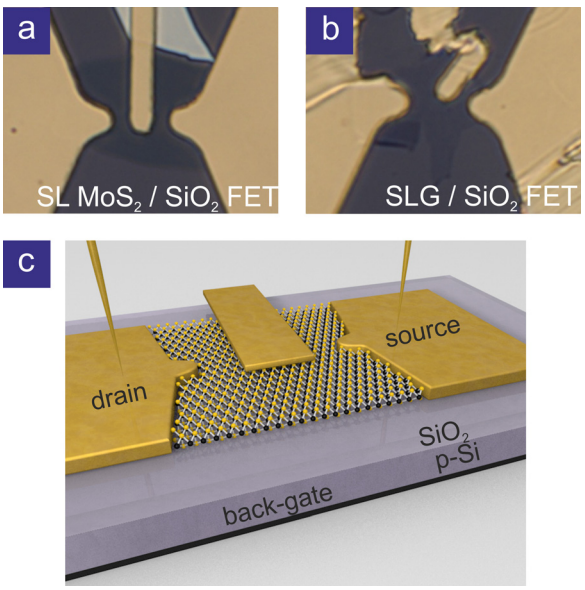

FIG. 1. Optical microscopy images of field effect devices based on (a) single layer MoS_2 and (b) single layer graphene. The electrical setup is schematically shown in (c). The third contact is not used and was kept floating during measurements.

a)Electronic address: marika.schleberger@uni-due.de.

characterization of the FETs before irradiation with respect to their output ($I_D(U_{DS})$) and transfer ($I_D(U_{GS})$) characteristics. Important physical properties as conductivity σ and mobility μ are directly derived from the experiment as follows:

$$\sigma = dI_D/dU_{DS}, \quad \text{and} \quad \mu = \frac{dI_D}{dU_{GS}} \times \frac{L}{WC_iU_{DS}}.$$

Here, I_D is the drain current, U_{GS} is the voltage between gate and source, U_{DS} is the voltage between drain and source, see Fig. 1. $C_i = \frac{\epsilon\epsilon_r}{d} = 3.837 \times 10^{-4}\,\mathrm{F/m^2}$ is the capacitance between the channel and the backgate per unit area, ϵ and ϵ_r are the dielectric constants of air and of the dielectric (SiO_2: $\epsilon_r = 3.9$), respectively, and d is the thickness of the oxide layer (90 nm). In addition, the charge carrier density can be directly derived from this data by

$$n_{e,h} = \frac{\sigma}{e\mu_n},$$

with e the elementary charge. Note, that μ and $\sigma(U_{GS} = 0\,\mathrm{V})$ are measured independently from each other, while $n(U_{GS} = 0\,\mathrm{V})$ is calculated from σ and μ.

The FET characteristics that we find are typical and comparable to literature data,[15,16] however, device performance is definitively below the reported record values, see below. In general, we found a great device-to-device variation with respect to transistor parameters (see Figs. 2 and 4). In addition, we observed that MoS_2 transistors show significant aging even if stored under N_2 atmosphere, while graphene devices appear to be stable for weeks. A significant hysteresis effect of MoS_2 transistors caused by the absorption of moisture on the surface was discussed by Late *et al.*[16] They showed that a top gate like Si_3N_4 can eliminate this effect to a large extent. A coated MoS_2 layer is, however, not desirable for the experiments performed in this work, where the MoS_2–FET is supposed to be exposed directly to the ion beam. Therefore, SLM FETs for this study have been prepared immediately before irradiation to avoid contamination problems.

In the fifth step, the samples were irradiated with 1.14 GeV ^{238}U in the UHV irradiation set-up at the M-branch of the swift heavy ion accelerator at the GSI in Darmstadt, Germany. For each type of FET, three different fluences φ were chosen: 4×10^{10}, 1.5×10^{11}, and 4×10^{11} ions/cm^2 (corresponding to 400, 1500, and 4000 ions/μm^2). In bulk materials, the radius of a typical SHI ion track (i.e., the permanently modified region) is about one nm. This means that at the chosen fluences only the last fluence may result in overlapping tracks while the lowest one definitely grants individual impacts. The projected range of the uranium ions at this energy is $\approx$46 μm.[17] It is therefore safe to assume that they completely pass the SiO_2 layer. The uranium ions themselves have thus no further influence on the electronic properties of the devices and any changes are consequences of the processes triggered by the projectiles.

For comparison, we irradiated additional SLM and SLG samples without electrical contacts with 4×10^{11} ions/cm^2 (high fluence) and under otherwise identical conditions chosen for the FETs. These samples were analyzed with atomic force microscopy (AFM, VECOO Dimension-3100; Nanosensors NCHR tips) in tapping mode and in the case of SLG also with Micro-Raman spectroscopy (LabRAM HR, Horiba Jobin Yvon), $E_L = 2.33\,\mathrm{eV}$, 1.96 eV, and 1.49 eV, $P_{Laser} \leq 1\,\mathrm{mW}$.

B. Results

First, we present the data for SLM FETs. The results for all three devices are shown in Fig. 2, where we have plotted the transfer characteristics, i.e., the drain current as a

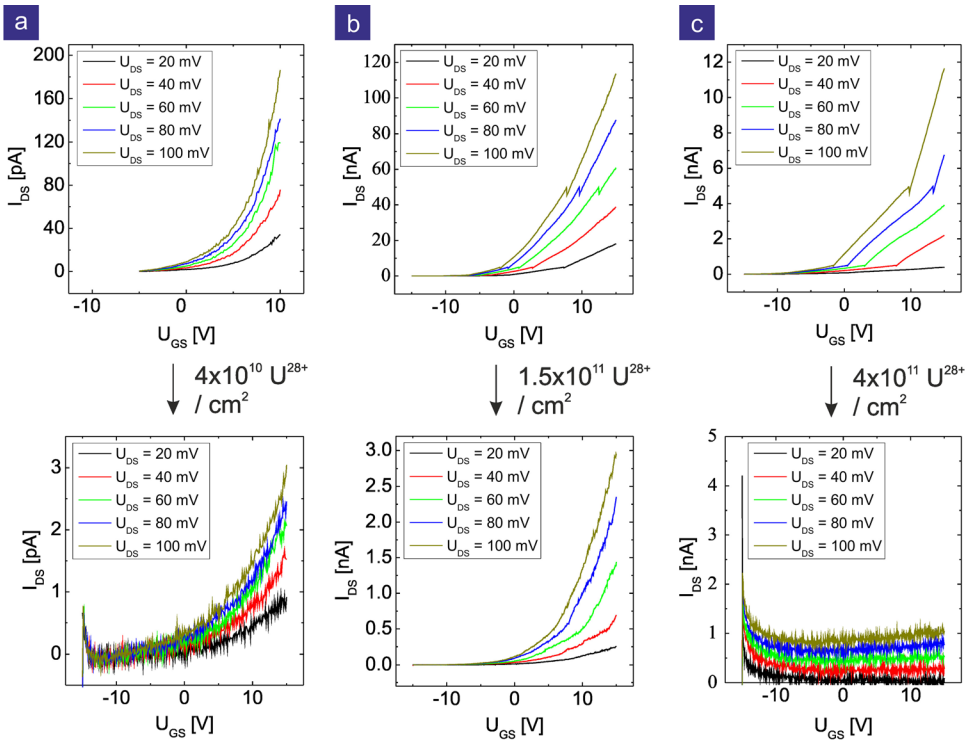

FIG. 2. Transfer characteristics of SLM FET devices. Upper panel shows $I_D(U_{GS})$ before irradiation for the three different devices. Lower panel shows $I_D(U_{GS})$ as recorded after irradiation with ^{238}U ions at a fluence of (a) 4×10^{10} ions/cm^2, (b) 1.5×10^{11} ions/cm^2, and (c) 4×10^{11} ions/cm^2, respectively.

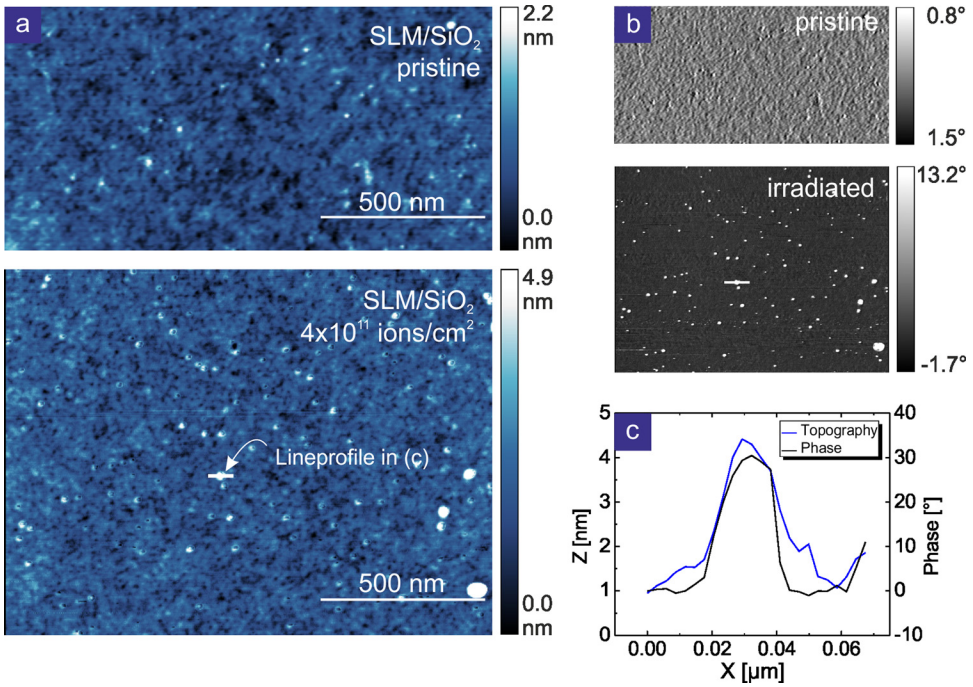

FIG. 3. (a) AFM topography image of SLM before (upper panel) and after irradiation (lower panel) with 4×10^{11} U ions/cm^2. After irradiation, the surface is covered with protrusions and small holes, the former can be clearly identified in the phase image (b). Their height is about a few nm, diameters can be as large as 50 nm.

function of the gate voltage. Before irradiation (upper panel), the SLM FETs show basically the same characteristics as reported in the literature. In our devices, amplification sets in at a gate voltage of about $U_{GS} = -4$ V (pinch-off). Typical values for mobility are $(2.5 \times 10^{-4} - 1.7 \times 10^{-1})$ cm^2/Vs and for charge carrier concentration $(9.8 \times 10^{11} - 2.5 \times 10^{13})$ n_e/cm^2.

After irradiation (Fig. 2, lower panel), those quantities show significant changes. At low fluences (a), we observe a decreased drain current by almost two orders of magnitude. Also for the intermediate fluence (b) the conductivity of the SLM FETs deteriorates. The corresponding drain current has decreased by ≈1.5 orders of magnitude with respect to the pristine SLM FET. Note however, that the device (b) was of higher quality to begin with, compared to the SLM FET exposed to the low fluence irradiation (a): The latter controls a current about three orders of magnitude less, see Fig. 2. For the highest fluence (c), the SLM FET is no longer operational. To verify this result, another device of this type was subjected to a high fluence irradiation. Also this second SLM FET was rendered non-functional by the irradiation.

Atomic force microscopy images of single layer MoS_2 exposed to the highest fluence show many randomly distributed hillocks (see Figs. 3(a) and 3(b), lower panels) which are not present on pristine samples (upper panels in Figs. 3(a) and 3(b)). Their apparent height depends strongly on the scanning parameters and they can be seen even more clearly in the corresponding phase images. These protrusions cover about 1.62% of the surface.

Second, we present the data for the SLG FETs. The results for all three devices are shown in Fig. 4, where we have plotted the conductivity as a function of the gate voltage. Before irradiation (black triangles), the SLG FETs show the ambipolar behaviour typical for graphene devices. All SLG FETs have excess carriers resulting in a *p*-type doping ranging from $(1.3 \times 10^{13}$–$1.4 \times 10^{13})$ ions/cm^2. Mobility values range from 243 to 390 cm^2/Vs for electrons, and for holes, we find 595–1198 cm^2/Vs.

After irradiation (Fig. 4, blue circles) with a low fluence (a) the mobility of the SLG FET increases significantly for holes as well as electrons, while the carrier density slightly decreases. For the intermediate fluence (b), the mobility decreases significantly while the carrier density slightly increases. Even after irradiation with the highest fluence (c), the SLG FET is still operational in contrast to the SLM FET. Carrier density has increased, hole mobility slightly decreased upon irradiation. Another SLG device was exposed to high fluence irradiation and remained operational as well.

Atomic force microscopy images of single layer graphene exposed to the highest fluence show many randomly distributed hillocks and rather large pits (see Fig. 5) which are not present on pristine samples. The overall appearance is similar to what has been found for SLM. The apparent height of the hillocks depends strongly on the scanning parameters. Because they can be seen even more clearly in the corresponding phase images, these data were analyzed to determine that protrusions cover about 1.09% of the surface.

In order to further analyze the nature of the induced defects in graphene, Raman spectroscopy was performed. This method has been proven to be a powerful tool to characterize defects in SLG.[18–21] The signature of defects is given by the double-resonant *D* and *D′* peaks at approximately 1350 cm^{-1} and 1620 cm^{-1} (Refs. 22 and 23). In Fig. 6, we show Raman spectra of a similar graphene flake as shown in Fig. 5, irradiated with 4×10^{11} ions/cm^2. Spectra have been taken with three different laser excitation energies enabling us to compare our results with the literature data from Ar^+ irradiated graphene (see Sec. II C).

C. Discussion

The data above indicate that the irradiation of 2D-FETs with SHI can have adverse effects: It can lead to inferior

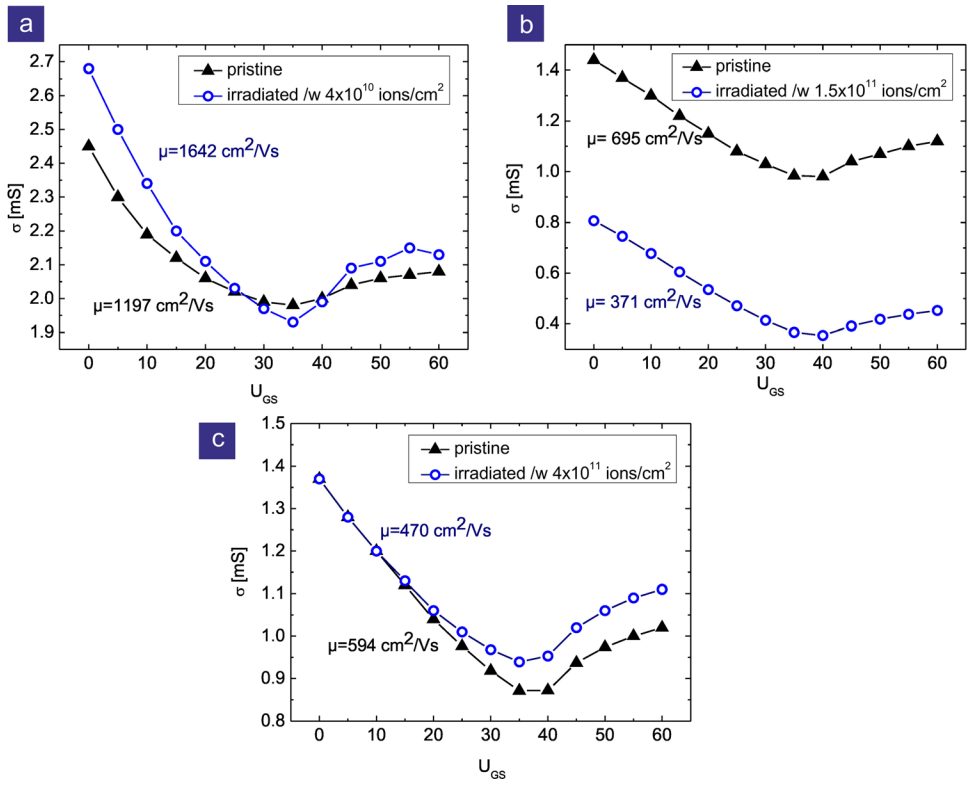

FIG. 4. Conductivity of three different SLG FETs as a function of gate voltage U_{GS} before (black triangles) and after irradiation (blue circles) with 4×10^{10} ions/cm^2, (b) 1.5×10^{11} ions/cm^2, and (c) 4×10^{11} ions/cm^2, respectively.

device performance (e.g., high fluences SLG FET) up to total destruction (SLM FET), but it can also cause an improved device performance (low fluences SLG FET). This immediately suggests that at least two counteracting mechanisms could play a role here. We propose that two relevant mechanisms are (1) doping and (2) defect creation. The latter seems to be straightforward as ion irradiation is known to cause structural defects, even in graphene[24–30] By using a combined scanning electron microscope/focused ion beam system, it has been shown that graphene possesses an enhanced resistance towards sputtering.[31] However, here, we have to keep in mind that the cross section for direct collisions of swift heavy ions with target atoms is negligible. In order for this mechanism to be in effect, we have to postulate that the electronic excitation caused by the SHI is the origin of the defect creation. This is in agreement with our finding here that SLM FETs are more easily destroyed than SLG FETs. In the latter material, the electronic energy will be spread very efficiently so that the energy density at a given time is too low to create large defects, while in MoS_2 (being a

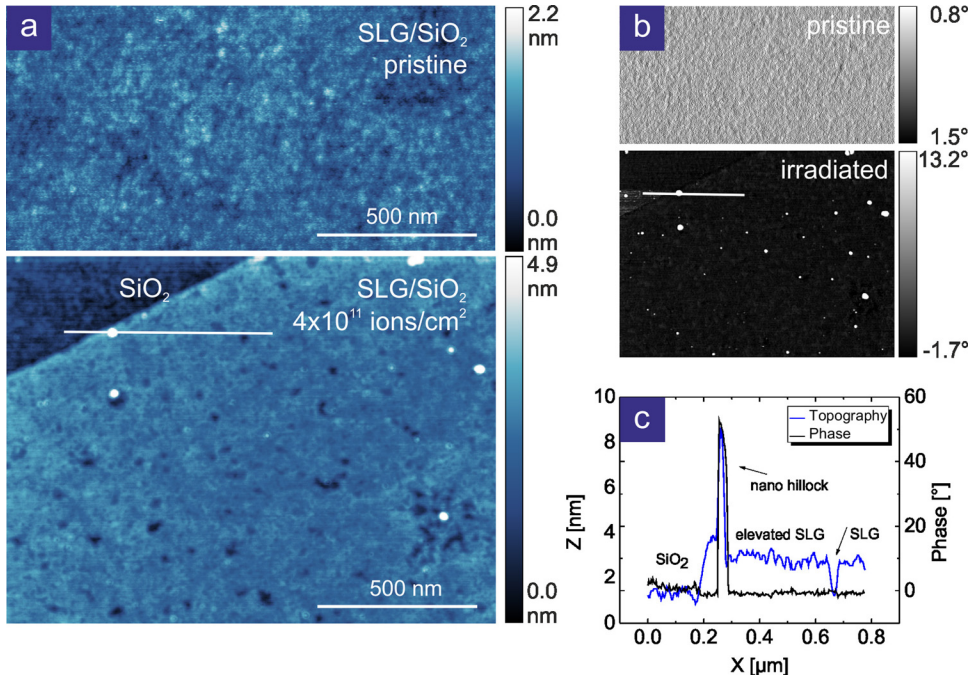

FIG. 5. (a) AFM topography image of pristine (upper panel) SLG and after irradiation (lower panel) with 4×10^{11} U ions/cm^2. After irradiation, the surface is covered with protrusions which can be clearly identified in the phase image (b). The hillocks height reaches 10 nm, the holes depth is limited to the apparent thickness of the SLG. The hillock diameter can be as large as 50 nm.

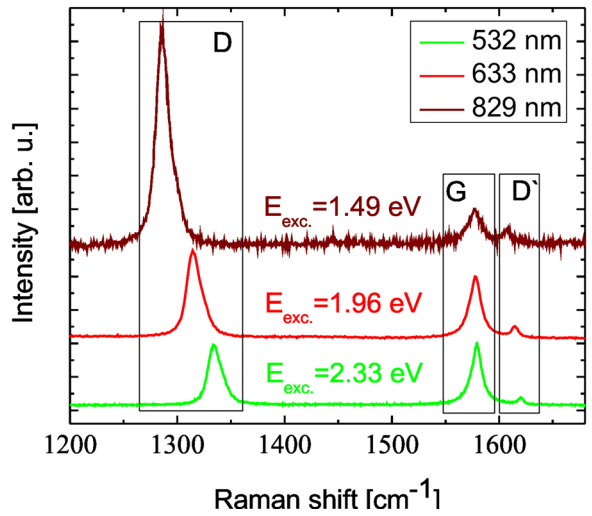

FIG. 6. Raman spectra of SLG after irradiation with 4×10^{11}U ions/cm^2 (high fluence) for three different excitation wave lengths. The *D* peak indicating irradiation induced defects is clearly present. The normalized $E_L^4(I_D/I_G)$ peak height ratio can be used to estimate the induced damage to the SLG sheet.

semiconductor), the electronic energy dissipation will be less rapid and significant damage will occur more easily. Any damage to the lattice will act as scattering center and will therefore result in reduced mobility.

The second mechanism, doping, will lead to an increased number of charge carriers and thus give rise to an enhanced conductivity (at a given mobility). Here, doping could be achieved in various ways: ions may either directly induce interstitials and vacancies or their interaction with the substrate gives rise to modifications of the graphene lattice. In this case, also substitutional doping would be possible in the following way.[32] After passing through the 2D material, the projectile enters the substrate where energy is deposited along its track. As the dielectric substrate material SiO_2 cannot dissipate the energy effectively, the primary electronic excitation is transferred to the lattice in a very small volume surrounding the trajectory. This heated zone is called a *thermal spike*[33] and causes material to be ejected at the impact sites in the near-surface regions.[34] This foreign material can be caught by graphene[35] and act as donor or acceptor, respectively. Substitutional doping by irradiation thus introduces additional charge carriers which might either increase the total charge carrier density or decrease it, depending on the type of carrier and the initial doping of the 2D material. Note that whether changes in carrier concentration are due to doping and/or to the removal of adsorbates cannot be distinguished at this point.

In the case of SLM FETs, doping by SHI irradiation seems to be only a minor effect and the deterioration of device performance with increasing fluence can be attributed solely to the increasing number of ion induced defects. The AFM images (Fig. 3) clearly show that the SLM sustains significant structural damage due to ion irradiation. At the highest fluence, ion tracks overlap and quite obviously material is ejected from the surface. The protrusions could be the remnants of this process.

In case of the SLG FETs (see Fig. 4), both mechanisms seem to play a role. Irradiation with SHI can increase the number of charge carriers (doping) but at the same time reduce their mean free path (defects). In order to further discuss our results, we focus in the following on the primary quantity which determines the performance of the SLG FET, i.e., the hole mobility.

Our experiment shows that the performance of an SLG FET with average mobility (see Fig. 4(a)) increases after low fluence irradiation. This would indicate that either scattering centers have been removed and/or electron density has increased by doping. Pristine exfoliated graphene on SiO_2 is usually *p*-doped due to adsorbates. The allegedly *reduced* hole density determined at $U_{GS} = 0$ is fully consistent with, e.g., substitutional doping, as the introduction of a given number of electrons from foreign atoms would compensate a corresponding number of holes and thus lead to an overall decreased holes density, while the hole conductivity at $U_{GS} = 0$ increases. Scattering centers related to doping at this fluence are still far enough apart: assuming point like defects the average distance l between to impacts is proportional to $\sqrt{1/\varphi}$ (Ref. 21) and thus amounts to 50 nm.

We also find that the SLG FET with a below-average performance (see Fig. 4(c)) remains more or less intact even after high fluence irradiation, i.e., the decrease in hole mobility is probably compensated by the increasing hole density. It is quite surprising that the degree of structural damage sustained by graphene seems to be comparable to that observed in MoS_2. Both AFM and Raman data show that the SLG is highly defective after high fluence irradiation, see Figs. 5 and 6. Nevertheless, the SLG FETs were still operational, proving the superior resistance of graphene devices to ionizing particle radiation as predicted using atomistic simulations.[36] The biggest effect of irradiation is observed if an SLG FET of below-average performance (see Fig. 4(b)) is irradiated with a medium fluence. Here, the decrease in mobility is the largest of all three irradiated SLG FETs and the very slight increase in carrier density can seemingly not compensate this effect.

Transport characteristics of FETs are governed by a variety of factors such as unintentional channel doping due to substrate interactions, environmental adsorbates, contacts or fabrication steps, as well as oxide thickness, channel width and length.[16,37–40] In devices where the latter is on the order of the depletion-layer widths of the source and drain junction, the carrier density does not necessarily remain constant at high gate voltages and short-channel effects must be considered.[41] In order to investigate these effects and to clarify the influence of ion irradiation induced contributions, experiments with dedicated devices are currently underway.

Finally, we discuss our Raman data. With respect to ion irradiation of graphene, it has been shown that point defects can be introduced in the graphene lattice most efficiently by low energy ion bombardment.[18] In order to estimate the density of defects which were created by SHI irradiation, we determined the amplitude ratio of the defect activated *D* mode to the *G* mode (I_D/I_G) multiplied by E_L^4 (where E_L is the Laser energy) to account for the energy dependence of I_D/I_G. Following the method from Refs. 18 and 19, we find for our sample an $E_L^4(I_D/I_G)$ ratio of ≈32 which corresponds

to $(7.5 \pm 2.3) \times 10^{11}$ defects/cm^2. Because the sample was irradiated with only 4×10^{11} ion/cm^2, defects induced by SHI seem to exceed single carbon atom displacements caused by 90 eV Ar^+ ions.

To test whether the defect creation in the SLG sheet is caused by the SHI projectile directly, we employed the TRIM code[17] to estimate the amount of sputtered atoms. Using the displacement energy for carbon atoms in the SLG lattice of 22 eV,[42] the sputtering yield of carbon atoms is found to be around 0.36 atoms/ion. Having irradiated the sample with 4×10^{11} ions/cm^2, about 1.4×10^{11} atoms/cm^2 should have been sputtered, resulting in a far lower defect concentration than found here by Raman spectroscopy. Thus, the dominant process of defect creation is not direct sputtering by the projectile but must be related to other mechanisms like a thermal spike[33] in the substrate or Coulomb explosion[43,44] in the 2D material. Note that the atom displacement energy for Mo and S atoms in MoS_2 of 7 eV (Ref. 45) is much lower than for carbon in graphene. Correspondingly, the calculated sputtering yields for MoS_2 show that about 0.6 MoS_2 atoms/ion and 1.0 S atoms/ion are directly displaced by the SHI. However, no experimental estimation of the defect concentration in SLM is currently available, preventing a direct comparison with graphene.

From this analysis, we conclude that the electronic excitation induced by the SHI in SLG, the substrate or both, is able to create large defects with a higher Raman cross section in graphene than Ar^+ ions. This unexpected effect will be studied in more detail in a forthcoming experiment.

D. Conclusions

We have shown that 2D FETs show significant changes with respect to output and transfer characteristics after irradiation with swift heavy ions. Devices may improve or deteriorate after irradiation, a finding which could be interpreted in terms of two mechanisms working in opposite directions. Especially our result that single layer graphene FETs can be improved with respect to conductivity might prove very interesting for applications. The doping mechanism could be used to increase the number of carriers without introducing too many scattering defects. It would be interesting to study this effect in devices which have been optimized before irradiation, e.g., by heating to remove adsorbates. This would also enable a more detailed study of the superior resistance of graphene FETs to ionizing particle irradiation in comparison to FETs based on MoS_2.

ACKNOWLEDGMENTS

We acknowledge financial support from the BMBF in the framework of the Research project *Modifikation von Systemen reduzierter Dimension durch Ionenbeschuss* and from the DFG in the framework of the Priority Program 1459 *Graphene* (O.O., N.S.), the SFB 616 *Energy dissipation on surfaces* (K.M.), and from the ERC under Grant No. 259286 (J.M.). We thank M. Freudenberg for graphics support.

[1]K. S. Novoselov, A. K. Geim, S. V. Morozov, D. Jiang, M. I. Katsnelson, I. V. Grigorieva, S. V. Dubonos, and A. A. Firsov, Nature **438**(7065), 197–200 (2005).
[2]K. I. Bolotin, K. J. Sikes, Z. Jiang, M. Klima, G. Fudenberg, J. Hone, P. Kim, and H. L. Stormer, Solid State Commun. **146**(9-10), 351–355 (2008).
[3]S. Morozov, K. Novoselov, M. Katsnelson, F. Schedin, D. Elias, J. Jaszczak, and A. Geim, Phys. Rev. Lett. **100**(1), 106602 (2008).
[4]Y.-M. Lin, K. A. Jenkins, A. Valdes-Garcia, J. P. Small, D. B. Farmer, and P. Avouris, Nano Lett. **9**(1), 422–426 (2009).
[5]B. Radisavljevic, A. Radenovic, J. Brivio, V. Giacometti, and A. Kis, Nat. Nanotechnol. **6**(3), 147–150 (2011).
[6]K. F. Mak, C. Lee, J. Hone, J. Shan, and T. F. Heinz, Phys. Rev. Lett. **105**(13), 136805 (2010).
[7]Y. Yoon, K. Ganapathi, and S. Salahuddin, Nano Lett. **11**(9), 3768–3773 (2011).
[8]F. Schwierz, Nat. Nanotechnol. **5**(7), 487–496 (2010).
[9]K. Kim, J.-Y. Choi, T. Kim, S.-H. Cho, and H.-J. Chung, Nature **479**(7373), 338–344 (2011).
[10]S. Das, H.-Y. Chen, A. V. Penumatcha, and J. Appenzeller, Nano Lett. **13**(1), 100–105 (2013).
[11]S. Bertolazzi, D. Krasnozhon, and A. Kis, ACS Nano **7**(4), 3246–3252 (2013).
[12]F. Aumayr, S. Facsko, A. S. El-Said, C. Trautmann, and M. Schleberger, J. Phys.: Condens. Matter **23**(39), 393001 (2011).
[13]*Swift Heavy Ions for Materials Engineering and Nanostructuring*, edited by D. K. Avashti and G. K. Mehta, Springer Series in Materials Science, Vol. 145 (2011).
[14]A. C. Ferrari, J. C. Meyer, V. Scardaci, C. Casiraghi, M. Lazzeri, F. Mauri, S. Piscanec, D. Jiang, K. S. Novoselov, S. Roth, and A. K. Geim, Phys. Rev. Lett. **97**(18), 187401 (2006).
[15]A. Venugopal, J. Chan, X. Li, C. W. Magnuson, W. P. Kirk, L. Colombo, R. S. Ruoff, and E. M. Vogel, J. Appl. Phys. **109**(10), 104511 (2011).
[16]D. J. Late, B. Liu, H. S. S. R. Matte, V. P. Dravid, and C. N. R. Rao, ACS Nano **6**(6), 5635–5641 (2012).
[17]J. F. Ziegler, M. D. Ziegler, and J. P. Biersack, Nucl. Instrum. Methods Phys. Res. B **268**(11–12), 1818–1823 (2010).
[18]M. M. Lucchese, F. Stavale, E. H M. Ferreira, C. Vilani, M. V. O. Moutinho, R. B. Capaz, C. A. Achete, and A. Jorio, Carbon **48**(5), 1592–1597 (2010).
[19]L. G. Cancado, A. Jorio, E. H. M. Ferreira, F. Stavale, C. A. Achete, R. B. Capaz, M. V. O. Moutinho, A. Lombardo, T. S. Kulmala, and A. C. Ferrari, Nano Lett. **11**(8), 3190–3196 (2011).
[20]A. Jorio, M. M. Lucchese, F. Stavale, E. H. Martins Ferreira, M. V. O. Moutinho, R. B. Capaz, and C. A. Achete, J. Phys. Condens. Matter **22**(33), 334204 (2010).
[21]E. H. Martins Ferreira, M. V. O. Moutinho, F. Stavale, M. M. Lucchese, R. B. Capaz, C. A. Achete, and A. Jorio, Phys. Rev. B **82**(12), 125429 (2010).
[22]C. Thomsen and S. Reich, Phys. Rev. Lett. **85**(24), 5214–5217 (2000).
[23]J. Maultzsch, S. Reich, and C. Thomsen, Phys. Rev. B **70**(15), 155403 (2004).
[24]E. H. Åhlgren, J. Kotakoski, and A. V. Krasheninnikov, Phys. Rev. B **83**(11), 115424 (2011).
[25]O. Lehtinen, J. Kotakoski, A. V. Krasheninnikov, A. Tolvanen, K. Nordlund, and J. Keinonen, Phys. Rev. B **81**(15), 153401 (2010).
[26]A. V. Krasheninnikov and K. Nordlund, J. Appl. Phys. **107**(7), 071301 (2010).
[27]S. Mathew, T. K. Chan, D. Zhan, K. Gopinadhan, A. Roy Barman, M. B. H. Breese, S. Dhar, Z. X. Shen, T. Venkatesan, and J. T. L. Thong, J. Appl. Phys. **110**(8), 084309 (2011).
[28]I. Deretzis, G. Piccitto, and A. La Magna, Nucl. Instrum. Methods Phys. Res. B **282**, 108–111 (2012).
[29]S. Zhao, J. Xue, Y. Wang, and S. Yan, Nanotechnology **23**, 285703 (2012).
[30]S. Akcöltekin, H. Bukowska, T. Peters, O. Osmani, I. Monnet, I. Alzaher, B. Ban d'Etat, H. Lebius, and M. Schleberger, Appl. Phys. Lett. **98**(10), 103103 (2011).
[31]J. J. Lopez, F. Greer, and J. R. Greer, J. Appl. Phys. **107**(10), 104326 (2010).
[32]O. Ochedowski, B. Kleine Bussmann, B. Ban d'Etat, H. Lebius, and M. Schleberger, Appl. Phys. Lett. **102**, 153103 (2013).
[33]M. Toulemonde, C. Dufour, and E. Paumier, Phys. Rev. B **46**(22), 14362–14369 (1992).
[34]E. Akcöltekin, T. Peters, R. Meyer, A. Duvenbeck, M. Klusmann, I. Monnet, H. Lebius, and M. Schleberger, Nat. Nanotechnol. **2**(5), 290–294 (2007).

[35]O. Ochedowski, S. Akcöltekin, B. Ban d'Etat, H. Lebius, and M. Schleberger, "Detecting swift heavy ion irradiation effects with graphene," Nucl. Instrum. Methods Phys. Res. B (in press).
[36]E. H. Åhlgren, J. Kotakoski, O. Lehtinen, and A. V. Krasheninnikov, Appl. Phys. Lett. **100**(23), 233108 (2012).
[37]F. Chen, J. Xia, D. K. Ferry, and N. Tao, Nano Lett. **9**(7), 2571–2574 (2009).
[38]S.-J. Han, Z. Chen, A. A. Bol, and Y. Sun, IEEE Electron Device Lett. **32**(6), 812–814 (2011).
[39]P. Joshi, H. E. Romero, A. T. Neal, V. K. Toutam, and S. A. Tadigadapa, J. Phys.: Condens. Matter **22**(33), 334214 (2010).
[40]K. Ganapathi, Y. Yoon, M. Lundstrom, and S. Salahuddin, IEEE Trans. Electron Devices **60**(3), 958–964 (2013).
[41]A. Alarcon, V.-H. Nguyen, S. Berrada, D. Querlioz, J. Saint-Martin, A. Bournel, and P. Dollfus, IEEE Trans. Electron Devices **60**(3), 985–991 (2013).
[42]J. C. Meyer, F. Eder, S. Kurasch, V. Skakalova, J. Kotakoski, H. J. Park, S. Roth, A. Chuvilin, S. Eyhusen, G. Benner, A. V. Krasheninnikov, and U. Kaiser, Phys. Rev. Lett. **108**, 196102 (2012).
[43]R. L. Fleischer, P. B. Price, and R. M. Walker, J. Appl. Phys. **36**, 3645 (1965).
[44]E. M. Bringa and R. E. Johnson, Phys. Rev. Lett. **88**, 165501 (2002).
[45]H.-P. Komsa, J. Kotakisko, S. Kurasch, O. Lehtinen, U. Kaiser, and A. V. Krasheninnikov, Phys. Rev. Lett. **109**, 035503 (2012).